Amphibolitization within the lower crust in the termination area of the Godzilla Megamullion, an oceanic core complex in the Parece Vela Basin

Amphibolitization within the lower crust in the termination area of the Godzilla Megamullion, an oceanic core complex in the Parece Vela Basin

Journal:	*Island Arc*
Manuscript ID:	IAR-10-0018.R2
Manuscript Type:	Research Article
Key words:	gabbroic rock, amphibolite, retrograde metamorphism, Godzilla Megamullion, amphibolitization, Parece Vela Basin

Revised manuscript

Amphibolitization within the lower crust in the termination area of the Godzilla Megamullion, an oceanic core complex in the Parece Vela Basin

Yumiko Harigane[a, *,**], Katsuyoshi Michibayashi[a, b], Yasuhiko Ohara[c,d]

[a]*Graduate school of Science and Technology, Shizuoka University, Shizuoka 422-8529, Japan*

[b]*Institute of Geosciences, Shizuoka University, Shizuoka 422-8529, Japan*

[c]*Hydrographic and Oceanographic Department of Japan, Tokyo 104-0045, Japan*

[d]*Institute for Research on Earth Evolution, Japan Agency for Marine-Earth Science and Technology, Kanagawa 236-0016, Japan*

*Corresponding author. Tel: +81-76-264-6539; Fax: +81-76-264-6545;

E-mail address: harigane@staff.kanazawa-u.ac.jp (Y. Harigane)

**Present address: Frontier Science Organization, Kanazawa University, Kakuma-machi, Kanazawa 920-1192, Japan

ABSTRACT

Gabbroic rocks and amphibolites collected from the KR03-1-D10 dredge site located on the West Arm Rise of the Godzilla Megamullion, close to the Parece Vela Rift, the Philippine Sea, during cruise KR03-1 of R/V *Kairei* revealed the occurrence of a high hydrothermal activity in the lower crust close to a paleo-ridge. In the gabbroic rocks, plagioclase compositions of both porphyroclasts and matrix were transformed into sodium-rich composition close to albite. Amphiboles are of secondary rather than igneous origin based on their microstructural occurrences. Both clinopyroxene and amphibole have roughly similar Mg# (= Mg/(Mg+Fe)). With respect to the amphibolites, anorthite contents of porphyroclasts and matrix plagioclase are relatively lower than those of the gabbroic rocks, whereas the chemical compositions of amphibole within the amphibolites are similar to those of amphibole within the gabbroic rocks. Therefore, amphibolites represent the product of retrograde metamorphism associated with hydrothermal alteration of the gabbroic body via the following reaction: clinopyroxene + plagioclase (calcic plagioclase) + fluid → amphibole + plagioclase (sodic plagioclase). The estimated temperatures of the amphibolites derived from the amphibole thermobarometer of Ernst & Liu (1998) range between ~700 and ~950°C, whereas those of the gabbroic rocks derived from the hornblende-plagioclase geothermometer of Holland & Blundy (1994) are between 650 and 840°C. Therefore, the hydrothermal alteration recorded in the gabbroic rocks possibly occurred under high-T conditions; the rocks were then metamorphosed to the amphibolites under retrogressive conditions or during retrogressive stage. The site KR03-1-D10 appears to correspond to the termination area of a detachment fault. Our study indicates that amphibolitization took place with various degrees of deformation there. Such amphibolitization has been reported only within ultramylonite in the breakaway area of the Godzilla Megamullion. Therefore, we argue that the hydrothermal activity could be higher in the termination area than in the breakaway area, resulting in intense amphibolitization regardless of deformation in the lower crust. It may imply that the hydrothermal activity increased as the Godzilla Megamullion developed as an oceanic core complex in the paleo-ridge.

Key words: gabbroic rock, amphibolite, retrograde metamorphism, Godzilla Megamullion, amphibolitization, Parece Vela Basin

INTRODUCTION

Oceanic core complexes (OCCs) are bathymetric features that were first identified along the Mid-Atlantic Ridge (e.g., Karson, 1990; Tucholke & Lin, 1994; Cann *et al*., 1997; Blackman *et al*., 1998; Tucholke *et al*., 1998). Based on morphological characteristics, OCCs usually occur close to the intersection of transform faults and the axis of a spreading ridge, and are characterized by a domal surface, corrugated parallel to the spreading direction, a high mantle Bouguer anomaly, and exposed lower crust and mantle material (e.g., Blackman *et al*., 1998; Tucholke *et al*., 1998). By analogy to continental metamorphic core complexes, it has been suggested that OCCs represent the exhumed footwalls of oceanic detachment faults (e.g., Karson, 1990; Dick *et al*., 1991, 2000, 2008; Cann *et al*., 1997; Blackman *et al*., 1998; Tucholke *et al*., 1998; Escartin *et al*., 2003; Ildefonse *et al*., 2007; MacLeod *et al*., 2009).

An extremely large OCC occurs within the extinct spreading axis (the Parece Vela Rift) in the Parece Vela Basin in the Philippine Sea, which is located on the southwest flank of the inactive S1 spreading segment (Fig. 1; Ohara *et al*., 2001). Topographic corrugations oriented perpendicular to the spreading segment are clearly visible across the surface of the complex, extending 55 km along the axis and 125 km perpendicular, covering an area about 10 times larger than the OCCs described at the Mid-Atlantic Ridge (Fig. 1; Ohara *et al*., 2001). Given its large size, Ohara *et al*. (2003b) named this OCC the Godzilla Megamullion.

Fault-related rocks derived from lithospheric mantle and lower oceanic crust occur on the surface of the Godzilla Megamullion (Harigane *et al*., 2005). Recently, Harigane *et al*. (2008) reported the earliest deformation recognized in this region, possibly related to initiation of the detachment fault, based on a study of deformed gabbroic rocks at dredge site KR03-01-D6 in the breakaway region (West Leg Ridge in Fig. 1). Harigane *et al*. (2008) revealed that the gabbroic shear zone subsequently evolved during progressive retrogression in association with hydration of the shear zone. In this paper, we focused on deformed gabbroic rocks sampled from the West Arm Rise in the termination area of the Godzilla Megamullion ~100 km away from the site KR03-01-D6 studied by Harigane *et al*. (2008) (Fig. 1). Although termination areas represent a key component in understanding how OCCs cease their development (Tucholke *et al*., 1998), no detailed studies have been done in the termination area of the

Godzilla Megamullion. We present results of detailed microstructural and petrological analyses for the deformed gabbroic rocks and amphibolites and discuss the occurrence of high hydrothermal activity within the lower crust in the termination area of the Godzilla Megamullion, giving a comparison between the degree of the retrograde metamorphism in the lower crust of the breakaway and termination areas of the Godzilla Megamullion.

GEOLOGICAL SETTING OF THE PARECE VELA BASIN

The Parece Vela Basin is an extinct backarc basin located between the Kyushu–Palau and the West Mariana Ridges (Fig. 1). The center of the basin is characterized by a N–S-trending chain of diamond-shaped depressions that define the Parece Vela Rift (Kasuga & Ohara, 1997). The spreading history of the basin involved two stages: an E–W rifting/spreading event from 26 to 20–19 Ma, followed by NE–SW spreading until 12 Ma (Okino *et al*., 1998, 1999; Ohara *et al*., 2001, 2003a, 2003b). The Parece Vela Rift became highly segmented during the second stage, resulting in the development of prominent fracture zones (Ohara *et al*., 2001).

DREDGE SAMPLES FROM THE TERMINATION AREA

The KR03-1-D10 dredge site is located at the West Arm Rise of the Godzilla Megamullion (Fig. 1), close to the Parece Vela Rift (Ohara *et al*., 2003b). The site appears to correspond to the termination area of a detachment fault. A total of 134 samples was obtained from this site during cruise KR03-1 of R/V *Kairei*, including 10 samples of basalt, 63 of gabbro, 15 of plagiogranite, and 46 of peridotite.

The retrieved gabbroic samples are not only so small, but also generally altered on the ocean floor. Therefore, we selected the ten least altered deformed samples of the 63 gabbroic rock samples for analysis. These are petrologically divided into four gabbroic rocks and six amphibolites (Tables 1 and 2). The four gabbroic rock samples range in size from 4.5 × 2.5 × 2.5 cm to 7.5 × 7 × 4.5 cm and display tectonic foliation. Sample KR03-1-D10-105 was analyzed in thin section oriented perpendicular to the foliation and parallel to the lineation (XZ sections), whereas the other three samples were analyzed in thin section with no particular orientation due to their cobble-sizes. The six amphibolite samples range in size from 3.5 × 2 × 2 cm to 10 × 8 × 3 cm. For one sample (KR03-1-D10-106), we were able to prepare a thin section oriented perpendicular to the foliation and parallel to the lineation (XZ section); for the other five samples, which were too small to enable the preparation of oriented thin sections, thin sections were prepared in random orientations.

SAMPLE CHARACTERISTICS

Microstructures of the gabbroic rock and amphibolite samples were studied by both optical microscopy and scanning electron microscopy (SEM; JEOL JSM6300) at Shizuoka University, Japan. The major element compositions of minerals were analyzed using an electron microprobe (JEOL JCXA-733) at Shizuoka University and an electron microprobe (JEOL JXA-8200) at the University of Tokyo, Japan. Operating conditions were as follows: probe current of 12 nA, accelerating voltage of 15 kV, and correction procedure after Bence & Albee (1968). Amphibole nomenclature and composition calculations follow Leake *et al*. (1997) and Holland & Blundy (1994), respectively.

Gabbroic rocks

The four gabbroic rock samples (KR03-1-D10-11, KR03-1-D10-103, KR03-1-D10-105 and KR03-1-D10-127) consist of plagioclase, clinopyroxene, amphibole, ilmenite, magnetite, apatite and chlorite (Table 1). These samples are characterized by mylonitic and porphyroclastic textures consisting dominantly of plagioclase porphyroclasts and lesser clinopyroxene and amphibole porphyroclasts in a fine-grained matrix of plagioclase and amphibole (Fig. 2a, b). They also display developed foliations defined by the tail of plagioclase and clinopyroxene/amphibole porphyroclasts (Fig. 2a, b).

Plagioclase occurs as coarse-grained porphyroclasts and fine-grained aggregates with amphibole in matrix, showing porphyroclastic texture (Fig. 2c). Plagioclase porphyroclasts (~2mm) show features of intracrystalline deformation such as undulose extinction and the formation of subgrains (Fig. 2c). Fine plagioclase grains in the matrix are polygonal and occur dominantly around the plagioclase porphyroclasts (Fig. 2c). The mean grain sizes of fine-grained plagioclase in the matrix vary between 40 and 100 μm (Figs. 2c, 3; Table 1). Clinopyroxene grains show partly undulose extinction and are replaced by secondary amphibole: brown and green hornblendes (Fig. 2d). Brown hornblende is found as a porphyroclast and a matrix mineral (Fig. 2d). It shows undulose extinction. A few green hornblendes occur at the rims of clinopyroxene grains (Fig. 2d), where they show no evidence of deformation (Fig. 2d). Chlorite also shows no deformation along secondary amphibole grains.

With respect to anorthite contents of plagioclase, plagioclase porphyroclasts and fine-grained matrix in these two samples (KR03-1-D10-11 and KR03-1-D10-127) share the similar range in composition ($An_{20–30}$; Fig. 4; Tables 1 and 3). In contrast, plagioclase compositions of both porphyroclast and matrix in the KR03-1-D10-105 sample and fine-grained matrix in sample KR03-1-D10-103 range widely from An_5 to An_{30} (Fig. 4; Tables 1 and 3). Plagioclase in these two samples (KR03-1-D10-11 and KR03-1-D10-127) show no compositional zoning, whereas those in samples of KR03-1-D10-103 and KR03-1-D10-105 show heterogeneous compositional zoning in the porphyroclasts and matrix.

Clinopyroxene represents augitic composition. The Mg# (= Mg/(Mg+Fe)) of clinopyroxene in the gabbroic rocks is 0.56–0.64 (Table 4).

Amphibole composition shows pargasite, edenite, magnesiohornbelnde (corresponding to brown hornblende) and actinolite (corresponding to green hornblende; Fig. 5a; Table 5). The Mg# varies between 0.31 and 0.62 (Fig. 5a; Table 5). Amphibole with similar compositions are frequently observed in oceanic metagabbros and amphibolites sampled from the KR03-1-D6 site in the Godzilla Megamullion (the West Leg Ridge; Harigane *et al*., 2008).

The hornblende–plagioclase geothermometer of Holland & Blundy (1994) has been applied for some pairs of brown hornblende (pargasite and magnesiohornblende) and fine-grained plagioclase matrix (An_{10-30}) within the gabbroic rocks. Pressure conditions were assumed to be 200 MPa that corresponds to 6-7 km of the depth in the oceanic crust. The results show that the estimated temperature was in the range between 650 and 840°C (Fig. 6a).

Amphibolites

The six amphibolites (KR03-1-D10-101, KR03-1-D10-106, KR03-1-D10-124, KR03-1-D10-129, KR03-1-D10-133 and KR03-1-D10-148; Fig. 2e, f; Table 2) show weakly or moderately developed foliations defined by oriented plagioclase and amphibole grains (Fig. 2e, f). The constituent minerals of the amphibolites consist of plagioclase, amphibole, ilmenite, magnetite, titanite, apatite, and chlorite (Table 2).

Plagioclase occurs dominantly as coarse-grained porphyroclasts in a fine-grained matrix that also contains small plagioclase grains (i.e., porphyroclastic texture; Fig. 2e, f). Plagioclase porphyroclasts (~2 mm) show features of intracrystalline deformation such as undulose extinction and subgrains with different intensities from one after another (Fig. 2e, f). Although plagioclase compositions vary in a range between An_0 and An_{30}, porphyroclasts and matrix grains within each sample are of similar composition (Fig. 4; Tables 2 and 3). Fine plagioclase grains in the matrix (typically 40–100 μm; Fig. 3) are polygonal where they occur around plagioclase porphyroclasts, and are unstrained.

Amphibole consists mainly of brown hornblende and minor green hornblende (Fig. 5b; Tables 2 and 5). Grains of brown hornblende show undulose extinction and are fine-grained (Fig. 2e, f). Green hornblende grains are unstrained. Amphibole grains have Mg# in the range of 0.38–0.66 and Si contents of 6.14–7.54 per formula unit (p.f.u.), corresponding to pargasite, edenite, magnesiohornblende and actinolite of Leake *et al.* (1997) (Fig. 5b; Table 5). These compositions are similar to those of amphibole within gabbroic rocks obtained from the same site (Fig. 5). Chlorite is unstrained and occurs near amphibole grains.

Since the hornblende-plagioclase geothermometer of Holland & Blundy (1994) is not applicable to sodic plagioclase ($<An_{20}$), we instead used the semi-quantitative amphibole thermobarometer of Ernst & Liu (1998) that can be applied to the natural metabasaltic assemblages that closely approached chemical equilibrium under crustal or uppermost mantle conditions. The estimated temperatures of the low-Mg# amphibolites ranges between ~700 and ~950°C (Fig. 6b).

DISCUSSION

Transformation of gabbros into amphibolites due to hydrothermal alteration

In the gabbroic rocks, plagioclase compositions of both porphyroclasts and matrix were transformed into sodium-rich composition close to albite composition ($An_{5\text{-}30}$; Fig. 4). Amphiboles are of secondary rather than igneous origin based on their microstructural occurrences (Fig. 2a-d). Clinopyroxene and amphibole have roughly similar Mg# values (Tables 4 and 5). The An contents of porphyroclasts and matrix in the gabbroic rocks (An_{5-30}) and amphibolites (An_{0-30}) overlap as clearly shown in Fig. 4, whereas amphibolites contain those of the plagioclase porphyroclasts and matrix that is lower than those of the gabbroic rocks (An_{5-30}; Fig. 4). On the other hand, the chemical compositions of the amphibole and mineral assemblages within the amphibolites are similar to those within the gabbroic rocks (Fig. 5; Tables 1 and 2).

Harigane *et al*. (2008) reported that the amphibolites recovered from the West Leg Ridge (Fig. 1) represent the product of retrograde metamorphism associated with hydrothermal alteration of the gabbroic body via the following reaction (Spear, 1981): clinopyroxene + plagioclase (calcic plagioclase) + fluid → amphibole + plagioclase (sodic plagioclase). Since the mineral assemblages of the gabbroic rocks in this study are similar to those of the gabbroic rocks reported by Harigane *et al*. (2008), this reaction can also be responsible for the transformation of gabbro into the amphibolite. It is also likely that the hydrothermal reaction would have occurred within the gabbroic rocks in this study.

The estimated temperatures of the amphibolites derived from the amphibole thermobarometer of Ernst & Liu (1998) range between ~700 and ~950°C (Fig. 6b), whereas those of the gabbroic rocks derived from the hornblende-plagioclase geothermometer of Holland & Blundy (1994) are between 650 and 840°C (Fig. 5a). In order to evaluate the estimated temperature in both Holland & Blundy (1994)'s and Ernst & Liu (1998)'s geothermometers, we also applied Ernst & Liu (1998)'s thermobarometer to the amphiboles in the gabbroic rocks; the result of estimated temperatures range between ~600 and ~900ºC (Fig. 6a). These temperature data in the gabbroic rocks have more or less the same high-temperature range. Although Ernst & Liu (1998)'s thermobarometer can be less accurate than the geothermometer of Holland & Blundy (1994) as reported by Ernst & Liu (1998), the estimated temperatures for the gabbroic rocks are grossly compatible between Ernst & Liu (1998)'s thermobarometer and Holland & Blundy (1994)'s geothermometer (Fig. 6a). Therefore, we argue that the hydrothermal alteration recorded in the gabbroic rocks possibly occurred under high-T conditions; the rocks were then metamorphosed to the amphibolites during retrogressive conditions.

Ocean-floor hydrothermal metamorphism in the Godzilla Megamullion

Many studies have investigated gabbros in ocean floor (e.g., Stakes & Vanko, 1986; Mével, 1987; Manning & MacLeod, 1996; Harigane *et al.*, 2008) and in ophiolites (e.g., Mével *et al.*, 1978; Girardeau & Mével, 1982; Berger *et al.*, 2005). One of the conclusions of these investigations is that an ocean-floor hydrothermal metamorphism is ubiquitous in the vicinity of a paleo-ridge (Berger *et al.*, 2005). In the Godzilla Megamullion, Harigane *et al.* (2008) showed that hydrothermal alteration resulted in retrograde metamorphism associated with deformation on the Fe-Ti oxide gabbroic body in the West Leg Ridge (Fig. 1). This gabbroic body occurred at the breakaway area of the detachment fault that exposed the Godzilla Megamullion (e.g., Ohara *et al.*, 2001).

This study showed that the gabbroic rocks in the termination area are characterized by porphyroclastic textures, which could have developed during shear deformation associated with the evolving detachment fault (Harigane *et al.*, 2008). Brown hornblende (i.e., pargasite, edenite and magnesiohonrblende) within these gabbroic rocks shows the features of plastic deformation, whereas green hornblende (i.e., actinolite) and chlorite shows no evidence of deformation (Fig. 2d). It indicates that higher-T hydrothermal alteration was associated with the deformation, whereas the lower-T hydrothermal alteration postdated the deformation in these gabbroic rocks. These microstructural features in the termination area are similar to those in the breakaway area documented by Harigane *et al.* (2008).

However, in contrast to the gabbroic rocks in the breakaway area, no correlation between grain size and An contents of plagioclase within the matrix have been found within the gabbroic rocks in the termination area (Fig. 4). Instead, variations in chemical compositions of plagioclase in both the porphyroclasts and matrices indicate intenser hydrothermal alteration than in the breakaway area documented by Harigane *et al.* (2008). Furthermore, the amphibolitization took place with various degrees of deformation in the termination area (Fig. 7), whereas such amphibolitization was only observed within the ultramylonite in the breakaway area (Harigane *et al.*, 2008). The estimated temperatures are relatively higher in the termination area than in the breakaway area. Consequently, we argue that the hydrothermal activity could be higher in the termination area than in the breakaway area, resulting in ubiquitous amphibolitization regardless of deformation in the lower crust (Fig. 7). It may imply that the hydrothermal activity increased as the Godzilla Megamullion was being developed in the paleo-ridge.

CONCLUSION

The four gabbroic rocks and six amphibolites obtained from the dredge site KR03-1-D10 in the West Arm Rise of the Godzilla Megamullion that appears to correspond to the termination area of a detachment fault. Microstructures of the gabbroic rocks are characterized by mylonitic and porphyroclastic textures consisting dominantly of plagioclase porphyroclasts and lesser clinopyroxene and amphibole porphyroclasts in a fine-grained matrix of plagioclase and amphibole, whereas amphibolites show weakly or moderately developed foliations defined by oriented plagioclase and amphibole grains. An contents of the porphyroclasts and matrix in the gabbroic rocks ($An_{5\text{-}30}$) and amphibolites ($An_{0\text{-}30}$) overlap. The amphibolites contain plagioclase porphyroclasts and matrix that have lower An contents than those of the gabbroic rocks ($An_{5\text{-}30}$). The chemical compositions of the amphibole and mineral assemblages within the amphibolites are similar to those of the amphibole and mineral assemblages within the gabbroic rocks. These resulted from the transformation of the gabbro into the amphibolites with the following hydrothermal reaction (Spear, 1981): clinopyroxene + plagioclase (calcic plagioclase) + fluid → amphibole + plagioclase (sodic plagioclase). The estimated temperatures of the amphibolites derived from the amphibole thermobarometer of Ernst & Liu (1998) and the hornblende-plagioclase geothermometer of Holland & Blundy (1994) show ~700-~950°C and 650-840°C, respectively. The hydrothermal alteration recorded in the gabbroic rocks possibly occurred under high-T conditions; the rocks were then metamorphosed to the amphibolites during retrogressive conditions. These microstructural features of gabbroic rocks and amphibolites in the termination area could have developed during shear deformation associated with the evolving detachment fault as proposed by Harigane *et al.* (2008). Furthermore, the amphibolitization took place with various degrees of deformation in the termination area. Hydrothermal activity could be high in the termination area, resulting in ubiquitous amphibolitization regardless of deformation in the lower crust.

ACKNOWLEDGEMENTS

We thank the captain and crew of R/V *Kairei*, the KR03-1 science party, Kyoko Okino, Teruaki Ishii and Toshiaki Masuda for their support and cooperation. We also thank Mitsuhiro Toriumi, who provided valuable suggestions that helped to improve an early draft of the manuscript. We also thank, the thorough comments by Hirokazu Maekawa, Graciano Yumul Jr., Georges Ceulenner and Rodolfo A. Tamayo Jr., for improving the paper. This study made use of analytical instruments housed at the Center for Instrumental Analysis, Shizuoka University. We thank Tatsu Kuwatani and Wataru Nishikanbara for their assistance in operating the JEOL JXA-8200 electron microprobe at the University of Tokyo. We thank Aaron Stallard for improving the English of the manuscript. We also thank Hideki Mori for technical assistance with the preparation of thin sections. This study was supported by student grants awarded to YH by the Graduate School of Science and Technology, Shizuoka University, and research grants awarded to KM (no. 19340148 and no. 16340151) and KO (no. 16340127) by the Japan Society for the Promotion of Science.

REFERENCES

Bence, A. E., & Albee, A. L., 1968. Empirical correction factors for the electron microanalysis of silicates and oxides. *Journal of Geology* **76**, 382-403.

Blackman, D. K., Cann, J. R., Janssen, B., & Smith, D. K., 1998. Origin of extensional core complexes: Evidence from the Mid-Atlantic Ridge at Atlantis Fracture Zone. *Journal of Geophysical Research* **103**, 21315–21333.

Berger, J., Femenias, O., Mercier, J. C. C., & Demaiffe, D., 2005. Ocean-floor hydrothermal metamorphism in the Limousin ophiolite (western French Massif Central): evidence of a rare preserved Variscan oceanic marker. *Journal of Metamorohic Geology* **23**, 795-812.

Cann, J. R., Blackman, D. K., Smith, D. K., et al., 1997. Corrugated slip surfaces formed at ridge-transform intersections on the Mid-Atlantic Ridge. *Nature* **385**, 329–332.

Dick, H. J. B., Natlamd, J. H., Alt, J. C., et al., 2000. A long in situ section of the lower ocean crust: results of ODP Leg 176 drilling at the Southwest Indian Ridge. *Earth* *and Planetary Science Letters* **179**, 31-51.

Dick, H. J. B., Schouten, H., Meyer, P. S., et al., 1991. Tectonic evolution of the Atlantis II Fracture Zone. *Proceedings of the Ocean Drilling Program Scientific Results* **118**, 359-398.

Dick, H. J. B., Tivey, M. A., & Tucholke, B. E., 2008. Plutonic foundation of a slow-spreading ridge segment: The oceanic core complex at Kane Megamullion, 23°30’N, 45°20’W. *Geochemistry Geophysics Geosystems* **9**, doi: 10.1029/2008GC002063.

Ernst, W. G., & Liu, J., 1998. Experimental phase-equilibrium study of Al- and Ti-contents of calcic amphibole in MORB—A semiquantitative thermobarometer. *American Mineralogist* **83**, 952–969.

Escartín, J., Mevel, C., MacLeod, C. J., & McCaig, A. M., 2003. Constraints on deformation conditions and the origin of oceanic detachments: The Mid-Atlantic Ridge core complex at 15°45'N. *Geochemistry Geophysics Geosystems* **4**, 1067, doi:10.1029/2001GC000278.

Girardeau, J., & Mevel, C., 1982. Amphibolitized sheared gabbros from ophiolites as indicators of the evolution the oceanic crust: Bay of Islands, Newfoundland. *Earth and Planetary Science Letters* **61**, 151-165.

Harigane, Y., Michibayashi, K. & Ohara, Y., 2005. Detachment faulting at the Godzilla Megamullion, Parece Vela Basin, Philippine Sea. *Eos Trans. AGU*, **86** (52), Fall Meetings Supplyment Abstract, T41D-1341.

Harigane, Y., Michibayashi, K., & Ohara, Y., 2008. Shearing within lower crust during progressive retrogression: Structural analysis of gabbroic rocks from the Godzilla Megamullion, an oceanic core complex in the Parece Vela backarc basin. *Tectonophysics* **457**, 183–196.

Holland, T. J. B., & Blundy, J. D., 1994. Non-ideal interactions in calcic amphiboles and their bearing on amphibole-plagioclase thermometry. *Contribution to Mineralogy and Petrology* **116**, 433-447.

Ildefonse, J., Blackman, D. K., John, B. E., et al., 2007. Oceanic core complexes and crustal accretion at slow-spreading ridges. *Geology* **35**, 623–626.

Karson, J. A., 1990. Seafloor spreading on the Mid-Atlantic Ridge: Implications for the structure of ophiolites and oceanic lithosphere produced in slow-spreading environments, in Ophiolites and Oceanic Crustal Analogues. *Proceedings of the Symposium "Troodos 1987"*, edited by J. Malpas et al., pp. 125–130, Geological Survey Department Nicosia, Cyprus.

Kasuga, S., & Ohara, Y., 1997. A new model of back-arc spreading in the Parece Vela Basin, northwest Pacific margin. *Island Arc* **6**, 316–326.

Leake, B.E., Woolley, A. R., Arps, C. E. S., et al., 1997. Nomenclature of amphiboles: Report of the Subcommittee on Amphiboles of the International Mineralogical Association Commission on New Minerals and Mineral Names. *American Mineralogist* **82**, 1019-1037.

MacLeod, C. J., Searle, R. C., Murton, B. J., et al., 2009. Life cycle of oceanic core complexes. *Earth and Planetary Science Letters* **287**, 3-4, 333-344.

Manning, C. E., & MacLeod, C. J., 1996, Fracture-controlled metamorphism of Hess Deep gabbros, site 894: constraints on the roots of mid-ocean hydrothermal systems at fast-spreading centers. *Proceedings of the Ocean Drilling Program Scientific Results* **147**, 189–212.

Mével, C., 1987. Evolution of oceanic gabbros from DSDP Leg 82: influence of the fluid phase on metamorphic crystallizations. *Earth and Planetary Science Letters* **83**, 67-79.

Mével, C., Caby, R., & Kienast, J. R., 1978. Amphibolite-facies conditions in the oceanic crust: example of amphibolitized flaser-gabbro and amphibolites from the Chenaillet ophiolite massif (Hautes Alpes, France). *Earth and Planetary Science Letters* **39**, 98–108.

Ohara, Y., Fujioka, K., Ishii, T., & Yurimoto, H., 2003a. Peridotites and gabbros from the Parece Vela backarc basin: Unique tectonic window in an extinct backarc spreading ridge. *Geochemistry Geophysics Geosystems* **4**, 1029, doi: 10.1029/2002GC000469.

Ohara, Y., Okino, K. Snow, J., & KR03-01 Shipboard Scientific Party, 2003b. Preliminary report of Kairei KR03-01 cruise: amagmatic tectonics and lithospheric composition of the Parece Vela Basin. *InterRidge News* **12**, 27–29.

Ohara, Y., Yoshida, T., & Kasuga, S., 2001. Giant megamullion in the Perece Vela Backarc basin. *Marine Geophysical Research* **22**, 47–61.

Okino, K., Kasuga, S., & Ohara, Y., 1998. A new scenario of the Parece Vela Basin genesis. *Marine Geophysical Research* **20**, 21–40.

Okino, K., Ohara, Y., Kasuga, S., & Kato, Y., 1999. The Philippine Sea: New survey results reveal the structure and the history of the marginal basins. *Geophysical Research Letters* **26**, 2287–2290.

Spear, F. 1981, An experimental study of hornblende stability and compositional variability in amphibolite. *American Journal of Science* **281**, 697-734.

Stakes, D., & Vanko, D. A., 1986. Multistage hydrothermal alteration of gabbroic rocks from the failed Mathematician ridge. *Earth and Planetary Science Letters* **79**, 75–92.

Tucholke, B. E. & Lin, J., 1994. A geological model for the structure of ridge segments in slow spreading ocean crust. *Journal of Geophysical Research* **99**, 11937-11958.

Tucholke, B. E., Lin, J., & Kleinrock, M. C., 1998. Megamullions and mullion structure defining oceanic metamorphic core complexes on the Mid-Atlantic Ridge. *Journal of Geophysical Research* **103**, 9857–9866.

FIGURE CAPTIONS

Fig. 1. The inset map shows the major bathymetric features of the Western Pacific Ocean. The black square shows the location of the site of the Godzilla Megamullion in the Parece Vela Basin. The main map is a bathymetric map of the Godzilla Megamullion, showing the dredge sites conducted during cruises KR03-1 and KH07-2. The site KR03-1-D10 (red star) is located on the northern portion of the West Arm Rise within the termination area of the Godzilla Megamullion. The site KR03-1-D6, located on the southern portion of the West Leg Ridge within the breakaway area of the Godzilla Megamullion, is also indicated. This study analyzed the gabbroic rocks and amphibolites from the site KR03-1-D10, making comparison with those from the site KR03-1-D6 (Harigane *et al*., 2008). The inactive spreading segments S1 and S2 (Ohara *et al*., 2001) are marked by thick red lines.

Fig. 2. Photomicrographs of microstructures within the gabbroic rocks and amphibolites collected from the site KR03-1-D10. Photomicrographs of microstructures within sample of (a) KR03-1-D10-11 and (b) KR03-1-D10-105. These textures show developed foliations defined by the tail of plagioclase and clinopyroxene/amphibole porphyroclast. Cross-polarized light. (c) Plagioclase porphyroclast and matrix in

KR03-1-D10-127. Cross-polarized light. Intracrystalline deformation on porphyroclast shows undulose extinction and subgrains. (d) Clinopyroxene porphyroclast with amphibole in KR03-1-D10-105. Clinopyroxene are replaced by brown hornblende and green hornblende. Plane polarized light. (e) Photomicrograph of the microstructure of amphibolite (KR03-1-D10-129). The porphyroclast shows features of plastic deformation, such as undulose extinction and subgrains. Cross-polarized light. (f) Photomicrograph of the microstructure of amphibolite (KR03-1-D10-106). These textures show developed foliations defined by the tail of plagioclase with fine-grained plagioclases and amphiboles. Cross-polarized light. Cpx: clinopyroxene, Amp: amphibole, Pl: plagioclase.

Fig. 3. Logarithmic grain-size distributions of fine-grained plagioclase grains within the gabbroic rocks and amphibolites. Outlines of plagioclase grains were traced from photomicrographs and back-scattered electron images, and shape parameters were measured using ImageJ software. This study measured a total of 208 to 483 plagioclase grains per sample. All of the distributions are log-normal. Triangles and numbers indicate the average grain size within each sample.

Fig. 4. Chemical compositions of plagioclase porphyroclasts (black diamonds) and fine grains in the matrix (white diamonds) for the gabbroic rocks and amphibolites. Anorthite content is calculated as Ca × 100 / (Ca + Na + K).

Fig. 5. Chemical composition of amphibole within the (a) gabbroic rocks and (b) amphibolites showing the plot of Mg# vs. Si. Estimates of cation contents and Fe^{3+} in all samples were made following Holland & Blundy (1994). The terminology and classification scheme are from Leake *et al*. (1997).

Fig. 6. Temperatures estimated by applying the hornblende–plagioclase geothermometer of Holland & Blundy (1994) to the gabbroic rocks and the semi-quantitative amphibole thermobarometer of Ernst & Liu (1998) to the gabbroic rocks and amphibolites.

Fig. 7. Schematic image showing a relative depth for the development of the gabbroic rocks and amphibolites, in the termination area (site KR03-1-D10) of the Godzilla Megamullion. The grey domain shows a gabbroic body. (a) The gabbroic body was partly deformed during shearing associated with the detachment fault, where intense amphibolitization occurred under high-T conditions at depth by hydrothermal alteration (black arrow). (b) The shear zone was further influenced by hydrothermal alteration under retrogressive conditions and relatively high-temperatures as low as 650 °C during uplift of the gabbroic body, resulting in ubiquitous occurrence of amphibolites.

Table 1. Petro-physical characteristics of gabbroic rocks.

Sample number	D10-11	D10-103	D10-105	D10-127
Microstructure	Mylonitic texture	Porphyroclastic texture	Mylonitic texture	Mylonitic texture
Mineral assemblage	Pl,Cpx, Amp (including Brown Hb and Green Hb), Ilm, Mt, Ap	Pl,Cpx, Amp (including Brown Hb and Green Hb), Ilm, Ap	Pl, Cpx, Amp (including Brown Hb and Green Hb), Ilm, Ap, Chl	Pl, Cpx, Amp (including Brown Hb and Green Hb), Ilm, Mt, Ap
Mineral mode(%)	Pl: 45.1 Cpx: 14.9 Amp: 30.3 Ilm+Mt: 8.1 Others: 1.6	Pl: 51.7 Cpx: 1.8 Amp: 32.9 Ilm: 7.4 Others: 6.2	Pl: 48.3 Cpx: 3.9 Amp: 32.8 Ilm+Mt: 5.8 Others: 9.2	Pl: 56.7 Cpx: 3.9 Amp: 27.1 Ilm+Mt: 11.6 Others: 0.7
Pl matrix average grain-size (μm)	46.9	-	93.8	64.1
Pl porphyroclast average An%	25.7	26.2	18.8	22.4
Pl matrix average An%	24.0	23.0	24.1	21.0

An%: anorthite contents, Pl: plagioclase, Cpx: clinopyroxene, Amp: amphibole, Hb: hornblende, Ilm: ilmenite, Mt: magnetite, Ap: apatite, Chl: chlorite.

Table 2. Petro-physical characteristics of amphibolites.

Sample number	D10-101	D10-106	D10-124	D10-129	D10-133	D10-148
Microstructure	Porphyrocla-stic texture	Mylonitic texture	Porphyrocla-stic texture	Porphyroc-lastic texture	Porphyrocla-stic texture	Porphyroclas-tic texture
Mineral assemblage	Pl, Amp (including Brown Hb and Green Hb), Ilm,Ap	Pl, Amp (including Brown Hb and Green Hb), Ilm, Chl, Ap	Pl, Amp (including Brown Hb), Ilm, Chl, Ap	Pl, Amp (including Brown Hb), Ilm, Ap	Pl, Amp (including Brown Hb and Green Hb), Ilm, Ttn	Pl, Amp (including Brown Hb), Ilm, Chl, Ap
Mineral mode(%)	Pl: 29.6 Amp: 69.3 Ilm: 0.1 Others: 1.0	Pl: 69.8 Amp: 20.6 Ilm: 5.9 Others: 3.7	-	-	-	Pl: 66.2 Amp: 28.9 Ilm: 2.2 Others: 2.7
Pl matrix average grain-size (μm)	42.1	97.3	83.7	-	-	40.0
Pl porphyroclast average An%	4.0	16.9	-	11.7	17.0	6.7
Pl matrix average An%	4.9	16.0	14.9	8.9	17.8	8.1

An%: anorthite contents, Pl: plagioclase, Amp: amphibole, Hb: hornblende, Ilm: ilmenite, Ttn: titanite, Ap: apatite, Chl: chlorite.

Table 3. Representative microprobe analyses of plagioclase in gabbroic rocks and amphibolites.

Rock type	gabbroic rock				amphibolite			
Sample No.	D10-11		D10-105		D10-106		D10-148	
Analysis No.	P-95	M-98	P-360	M-362	P-269	M-270	P-47	M-45
wt%								
SiO_2	60.86	62.29	61.00	62.76	62.89	63.75	67.65	67.62
TiO_2	0.07	0.02	0.07	0.02	0.04	0.01	0.00	0.02
Al_2O_3	23.81	23.02	24.39	23.10	23.06	22.42	20.13	20.05
FeO	0.16	0.24	0.11	0.08	0.08	0.08	0.15	0.21
MnO	0.02	0.00	0.00	0.01	0.00	0.00	0.00	0.02
MgO	0.00	0.02	0.03	0.01	0.01	0.00	0.00	0.01
CaO	5.59	4.70	6.16	4.84	4.24	3.56	1.11	1.15
Na_2O	8.26	8.86	7.83	8.57	9.13	9.75	11.01	10.94
K_2O	0.26	0.18	0.16	0.18	0.27	0.09	0.05	0.21
Cr_2O_3	0.00	0.04	0.00	0.00	0.02	0.00	0.00	0.02
NiO	0.06	0.01	0.00	0.00	0.00	0.01	0.00	0.00
V_2O_3	0.01	0.00	0.00	0.00	0.00	0.00	0.01	0.01
Total	99.10	99.38	99.75	99.57	99.74	99.67	100.11	100.26
Cations / O	8	8	8	8	8	8	8	8
Si	2.731	2.779	2.717	2.788	2.791	2.825	2.959	2.957
Ti	0.002	0.001	0.002	0.001	0.001	0.000	0.000	0.001
Al	1.259	1.210	1.280	1.209	1.206	1.171	1.037	1.033
Fe*	0.006	0.009	0.004	0.003	0.003	0.003	0.006	0.008
Mn	0.001	0.000	0.000	0.000	0.000	0.000	0.000	0.001
Mg	0.000	0.001	0.002	0.000	0.000	0.000	0.000	0.001
Ca	0.269	0.225	0.294	0.231	0.201	0.169	0.052	0.054
Na	0.718	0.766	0.676	0.738	0.786	0.838	0.934	0.928
K	0.015	0.010	0.009	0.010	0.015	0.005	0.003	0.011
Cr	0.000	0.001	0.000	0.000	0.001	0.000	0.000	0.001
Ni	0.002	0.001	0.000	0.000	0.000	0.000	0.000	0.000
V	0.000	0.000	0.000	0.000	0.000	0.000	0.000	0.000
Total	5.003	5.003	4.984	4.980	5.004	5.011	4.991	4.995
An%	26.8	22.4	30.0	23.6	20.1	16.7	5.3	5.4

Fe* is calculated by all Fe^{2+}. P- and M- are porphyroclast and matrix, respectively.

478

Table 4. Representative microprobe analyses of clinopyroxene in gabbroic rocks.

Sample No.	D10-11	D10-103	D10-105	D10-127
Analysis No.	CPX-77	CPX-52	CPX-67	CPX-51
wt%				
SiO_2	51.28	51.81	51.38	51.28
TiO_2	0.31	0.74	0.46	0.57
Al_2O_3	0.94	1.47	1.04	1.23
FeO	13.67	12.11	12.22	14.19
MnO	0.57	12.27	0.46	0.50
MgO	10.51	0.36	12.44	10.33
CaO	21.33	20.31	21.71	21.52
Na_2O	0.56	0.69	0.59	0.55
K_2O	0.01	0.00	0.02	0.00
Cr_2O_3	0.00	0.00	0.07	0.01
NiO	0.00	0.00	0.06	0.00
V_2O_3	0.00	0.00	0.06	0.01
Total	99.18	99.76	100.51	100.19
Cations / O	6	6	6	6
Si	1.976	2.061	1.945	1.961
Ti	0.009	0.022	0.013	0.016
Al	0.042	0.069	0.046	0.056
Fe*	0.440	0.403	0.387	0.454
Mn	0.019	0.413	0.015	0.016
Mg	0.604	0.021	0.702	0.589
Ca	0.881	0.866	0.881	0.882
Na	0.042	0.053	0.043	0.041
K	0.000	0.000	0.001	0.000
Cr	0.000	0.000	0.002	0.000
Ni	0.000	0.000	0.002	0.000
V	0.000	0.000	0.002	0.000

Total	4.013	3.908	4.039	4.015
Mg/Mg+Fe	0.58	0.64	0.64	0.56
Wo	45.7	43.4	44.7	45.8
En	31.4	36.5	35.7	30.6
Fs	22.9	20.2	19.6	23.6

Fe* is calculated by all Fe2+.

Table 5. Representative microprobe analyses of amphibole in gabbroic rocks and amphibolites.

Rock type	gabbroic rock				amphibolite		
Sample No.	D10-11		D10-105		D10-106		D10-148
Analysis No.	Amp-104 Pg	Amp-90 Hb	Amp-32 Pg	Amp-55 Act	Amp-261 Pg	Amp-49 Act	Amp-24 Hb
wt%							
SiO_2	40.17	44.59	40.24	52.65	43.95	49.98	47.23
TiO_2	3.13	2.51	3.56	0.35	2.70	1.05	1.58
Al_2O_3	9.80	7.38	10.50	2.35	7.40	2.68	5.82
FeO	19.87	20.36	19.34	16.36	19.24	20.33	17.36
MnO	0.33	0.40	0.23	0.25	0.37	0.47	0.29
MgO	9.11	8.49	9.24	12.48	10.28	11.96	12.26
CaO	10.84	10.30	10.67	11.97	10.25	8.52	10.93
Na_2O	3.04	2.08	3.25	0.58	3.09	1.17	2.06
K_2O	0.61	0.48	0.49	0.05	0.28	0.06	0.25
Cr_2O_3	0.01	0.00	0.06	0.00	0.00	0.00	0.01
NiO	0.03	0.05	0.03	0.00	0.00	0.03	0.02
V_2O_3	0.00	0.00	0.00	0.00	0.00	0.00	0.10
Total	96.94	96.64	97.61	97.04	97.56	96.25	97.91
Cations / O	23	23	23	23	23	23	23
Si	6.230	6.833	6.155	7.765	6.686	7.548	7.016
Al^{iv}	1.770	1.167	1.845	0.235	1.314	0.452	0.984
Al^{vi}	0.021	0.165	0.047	0.174	0.013	0.025	0.034
Ti	0.364	0.289	0.410	0.039	0.309	0.119	0.177
Fe^{3+}	0.152	0.210	0.265	0.016	0.075	0.144	0.196
Mg	2.107	1.939	2.106	2.744	2.332	2.692	2.715
Fe^{2+}	2.424	2.399	2.209	2.001	2.372	2.422	1.960
Mn	0.044	0.052	0.030	0.031	0.048	0.060	0.036
Ca	1.800	1.691	1.747	1.892	1.671	1.379	1.739
Na	0.912	0.618	0.963	0.166	0.913	0.342	0.594

K	0.120	0.095	0.096	0.009	0.055	0.011	0.047
Cr	0.001	0.000	0.007	0.000	0.000	0.000	0.001
Ni	0.004	0.006	0.004	0.000	0.000	0.004	0.003
V	0.000	0.000	0.000	0.000	0.000	0.000	0.012
Total	15.95	15.46	15.88	15.07	15.79	15.20	15.51
(Na+K)A	0.95	0.46	0.88	0.07	0.79	0.20	0.51
Mg/Mg+Fe	0.47	0.45	0.49	0.58	0.50	0.53	0.58

Estimate of Fe^{3+} follows Holland & Blundy (1994).

Pg:Pargasite, Hb:Hornblende, Act: Actinolite.

Figure 1

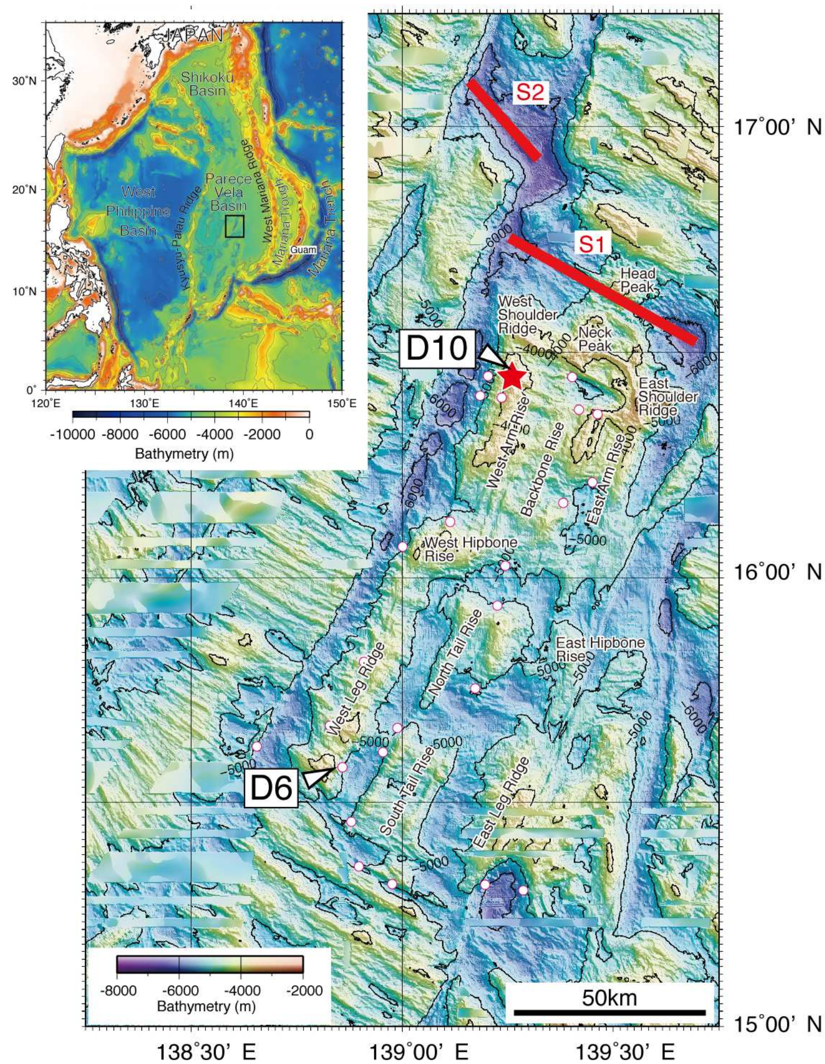

Figure 1. Harigane et al.

Fig. 1. The inset map shows the major bathymetric features of the Western Pacific Ocean. The black square shows the lacation of the site of the Godzilla Megamullion in the Parece Vela Basin. The main map is a bathymetric map of the Godzilla Megamullion, showing the dredge sites conducted during cruises KR03-01 and KH07-02. The site KR03-01-D10 (red star) is located on the northern portion of the West Arm Rise within the termination area of the Godzilla Megamullion. The site KR03-01-D6, located on the southern portion of the West Leg Ridge within the breakaway area of the Godzilla Megamullion, is also indicated. This study analyzed the gabbroic rocks and amphibolites from the site KR03-01-D10, making comparison with those from the site KR03-01-D6 (Harigane et al., 2008). The inactive spreading segments S1 and S2 (Ohara et al., 2001) are marked by thick red lines.
209x283mm (150 x 150 DPI)

Figure 2

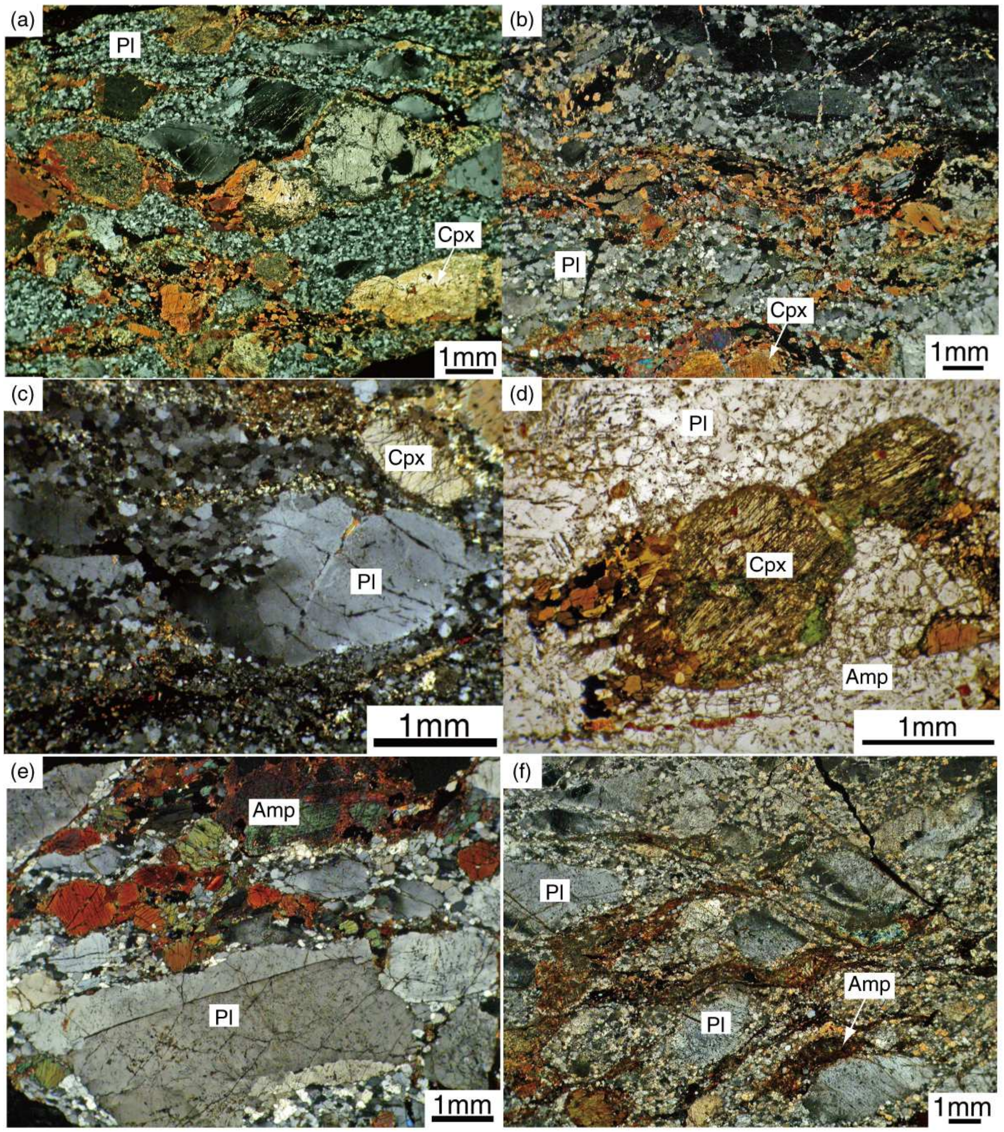

Figure 2 Harigane et al.

Fig. 2. Photomicrographs of microstructures within the gabbroic rocks and amphibolites collected from the site KR03-01-D10. Photomicrographs of microstructures within sample of (a) KR03-01-D10-11 and (b) KR03-01-D10-105. These textures show developed foliations defined by the tail of plagioclase and clinopyroxene/amphibole porphyroclast. Cross-polarized light. (c) Plagioclase porphyroclast and matrix in KR03-01-D10-127. Cross-polarized light. Intracrystalline deformation on porphyroclast shows undulose extinction and subgrains. (d) Clinopyroxene porphyroclast with amphibole in KR03-01-D10-105. Clinopyroxene are replaced by brown hornblende and green hornblende. Plane polarized light. (e) Photomicrograph of the microstructure of amphibolite (KR03-01-D10-129). The porphyroclast shows features of plastic deformation, such as undulose extinction and subgrains. Cross-polarized light. (f) Photomicrograph of the microstructure of amphibolite (KR03-01-D10-106). These textures show developed foliations defined by the tail of plagioclase with fine-grained plagioclases and amphiboles. Cross-polarized light. Cpx: clinopyroxene, Amp:

amphibole, Pl: plagioclase.
203x243mm (150 x 150 DPI)

Figure 3

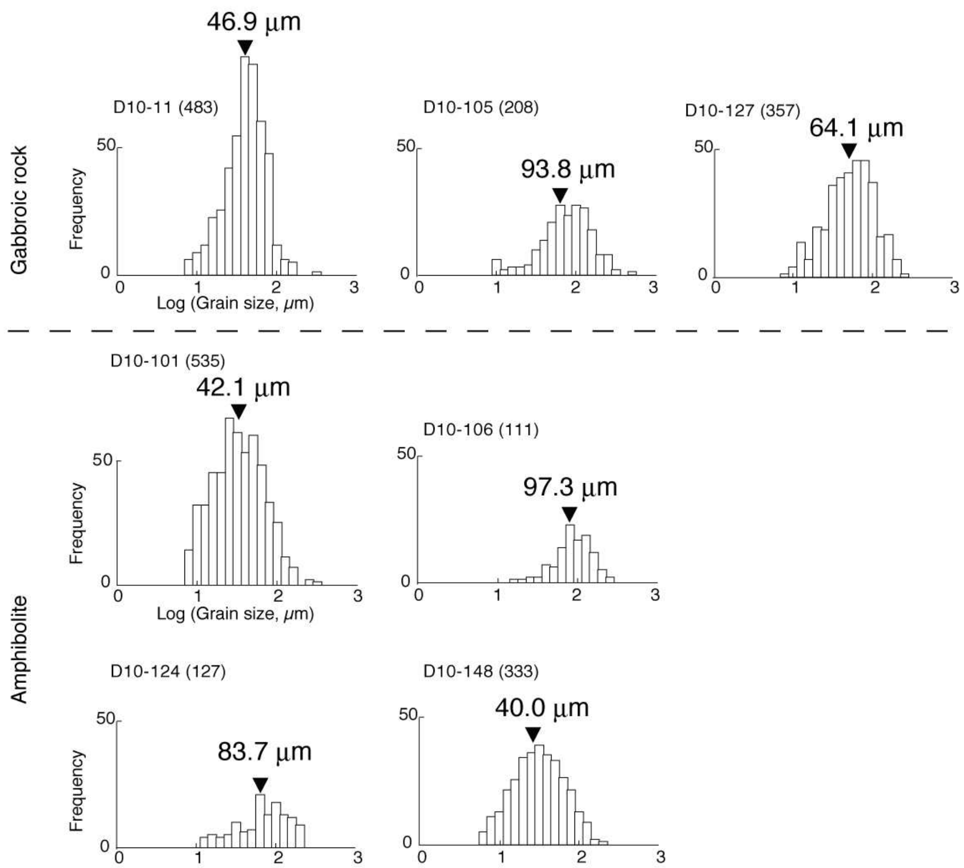

Figure 3 Harigane et al.

Fig. 3. Logarithmic grain-size distributions of fine-grained plagioclase grains within the gabbroic rocks and amphibolites. Outlines of plagioclase grains were traced from photomicrographs and back-scattered electron images, and shape parameters were measured using ImageJ software. This study measured a total of 208 to 483 plagioclase grains per sample. All of the distributions are log-normal. Triangles and numbers indicate the average grain size within each sample.
202x201mm (150 x 150 DPI)

Figure 4

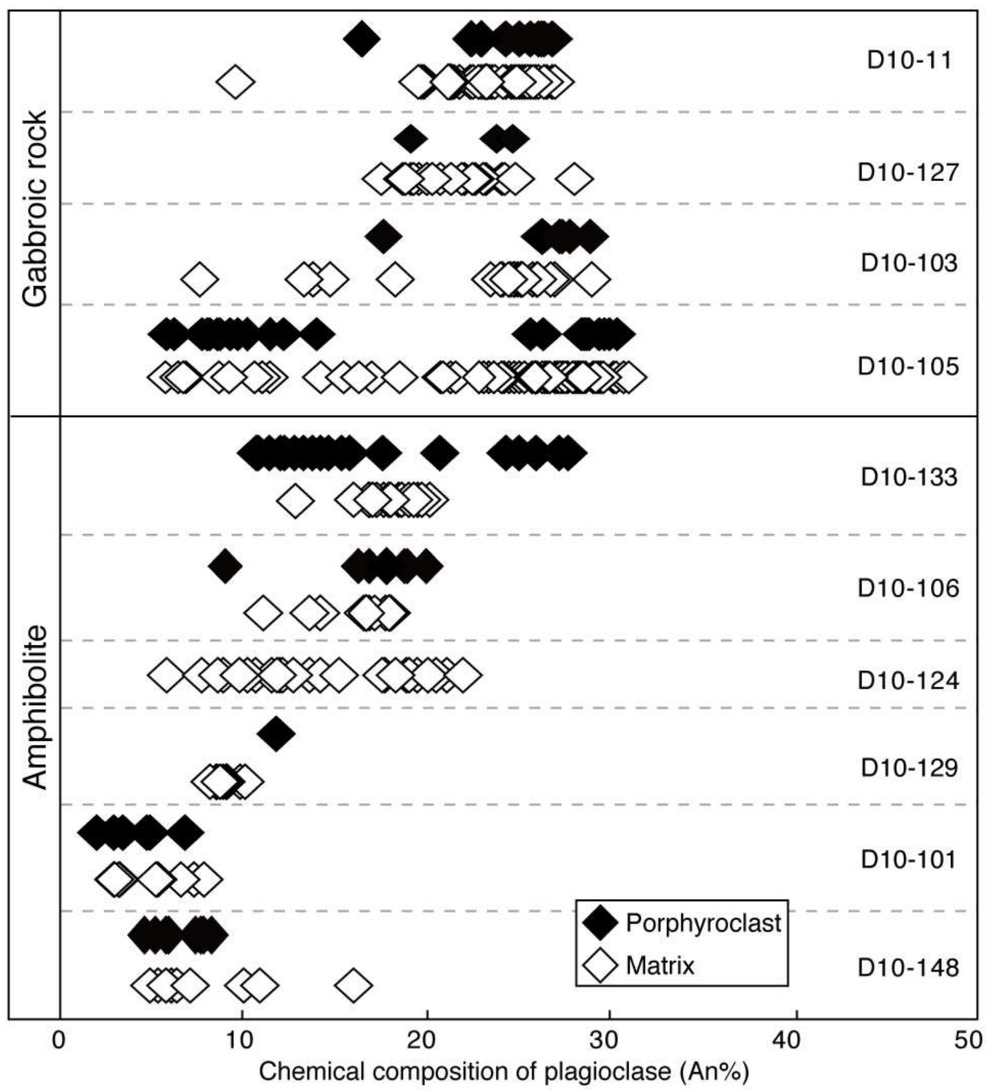

Figure 4 Harigane et al.

Fig. 4. Chemical compositions of plagioclase porphyroclasts (black diamonds) and fine grains in the matrix (white diamonds) for the gabbroic rocks and amphibolites. Anorthite content is calculated as Ca × 100 / (Ca + Na + K).
165x198mm (150 x 150 DPI)

Figure 5

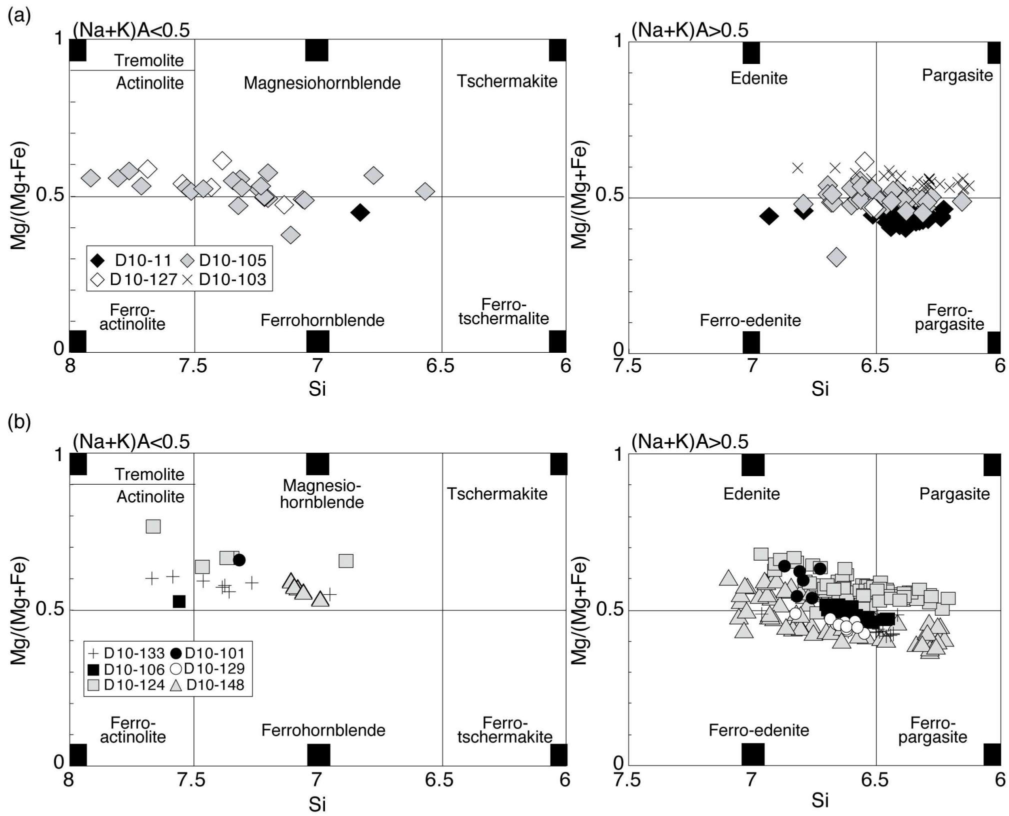

Figure 5 Harigane et al.

418x395mm (150 x 150 DPI)

Figure 6

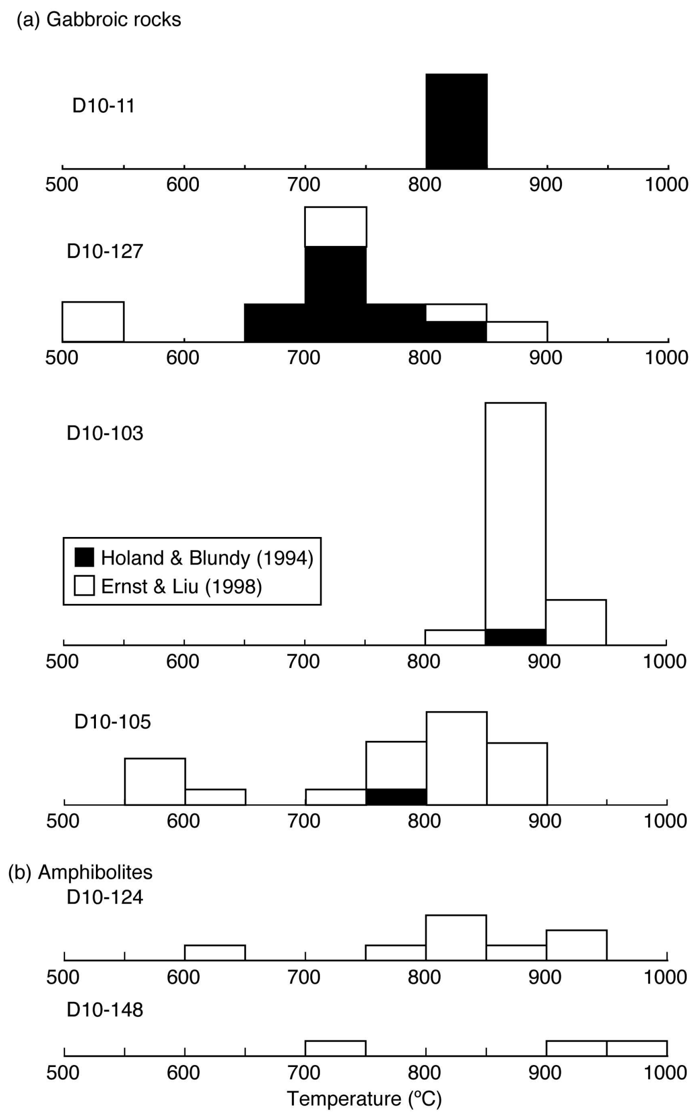

Figure 6 Harigane et al.

164x252mm (300 x 300 DPI)

Figure 7

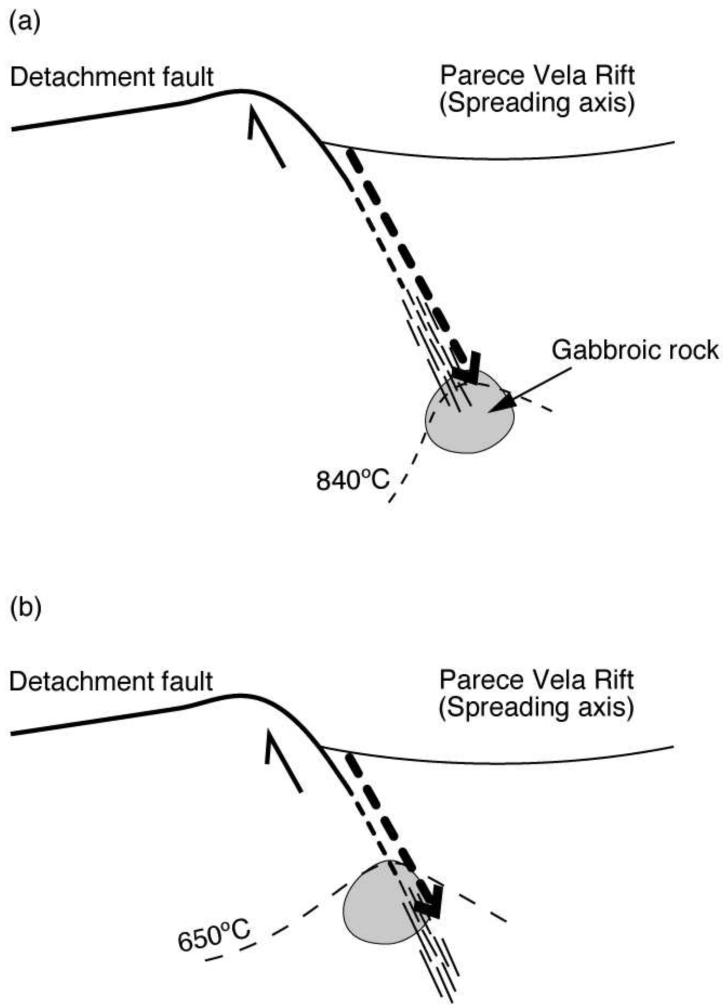

Figure 7 Harigane et al.

Fig. 7. Schematic image showing a relative depth for the development of the gabbroic rocks and amphibolites, in the termination area (site KR03-01-D10) of the Godzilla Megamullion. The grey domain shows a gabbroic body. (a) The gabbroic body was partly deformed during shearing associated with the detachment fault, where intense amphibolitization occurred under high-T conditions at depth by hydrothermal alteration (black arrow). (b) The shear zone was further influenced by hydrothermal alteration under retrogressive conditions and relatively high-temperatures as low as 650 °C during uplift of the gabbroic body, resulting in ubiquitous occurrence of amphibolites.
132x187mm (150 x 150 DPI)